



Contents lists available at SciVerse ScienceDirect

Spectrochimica Acta Part A: Molecular and Biomolecular Spectroscopy

journal homepage: www.elsevier.com/locate/saa

Hetero-binuclear near-infrared (NIR) luminescent Zn–Nd complexes self-assembled from the benzimidazole-based ligands

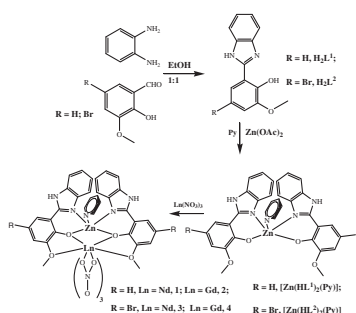
Dan Zou^{a,b}, Weixu Feng^{a,*}, Guoxiang Shi^{a,b}, Xingqiang Lü^{a,b,c,*}, Zhao Zhang^{a,b}, Yao Zhang^{a,b}, Han Liu^{a,b}, Daidi Fan^{a,b}, Wai-Kwok Wong^d, Richard A. Jones^e^a Shaanxi Key Laboratory of Degradable Medical Material, Northwest University, Xi'an 710069, Shaanxi, China^b Shaanxi Key Laboratory of Physico-inorganic Chemistry, Northwest University, Xi'an 710069, Shaanxi, China^c Fujian Institute of Research on the Structure of Matter, Chinese Academy of Science, Fuzhou 350002, Fujian, China^d Department of Chemistry, Hong Kong Baptist University, Waterloo Road, Kowloon Tong, Hong Kong, China^e Department of Chemistry and Biochemistry, The University of Texas at Austin, 1 University Station A5300, Austin, TX 78712-0165, United States

HIGHLIGHTS

- ▶ Hetero-binuclear Zn–Ln (Ln = Nd or Gd) arrayed complexes assembled from the benzimidazole-based ligands.
- ▶ Heavy-atom effect.
- ▶ Enhancement of near-infrared luminescent properties.

GRAPHICAL ABSTRACT

Hetero-binuclear complexes $[\text{ZnLn}(\text{HL}^1)_2(\text{Py})(\text{NO}_3)_3]$ (Ln = Nd, **1**; Ln = Gd, **2**) and $[\text{ZnLn}(\text{HL}^2)_2(\text{Py})(\text{NO}_3)_3]$ (Ln = Nd, **3**; Ln = Gd, **4**) were obtained from two benzimidazole-based ligands H_2L^1 and H_2L^2 , respectively. The sensitization and energy transfer for the NIR luminescence of the Nd^{3+} ions in the two Zn–Nd complexes (**1** and **3**) were discussed.



ARTICLE INFO

Article history:

Received 24 May 2012

Received in revised form 30 July 2012

Accepted 21 August 2012

Available online 28 August 2012

Keywords:

Zn–Ln arrayed benzimidazole-based complexes

UV–vis absorption

Visible and NIR luminescence

Sensitization and energy transfer

ABSTRACT

With the compound $[\text{Zn}(\text{HL}^1)_2(\text{Py})]$ ($\text{H}_2\text{L}^1 = 2-(1\text{H-benzo[d]imidazol-2-yl})-6\text{-methoxyphenol}$), $\text{Py} = \text{pyridine}$ or $[\text{Zn}(\text{HL}^2)_2(\text{Py})]$ ($\text{H}_2\text{L}^2 = 2-(1\text{H-benzo[d]imidazol-2-yl})-4\text{-bromo-6-methoxyphenol}$) as the precursor, complexes $[\text{ZnLn}(\text{HL}^1)_2(\text{Py})(\text{NO}_3)_3]$ (Ln = Nd, **1**; Ln = Gd, **2**) or $[\text{ZnLn}(\text{HL}^2)_2(\text{Py})(\text{NO}_3)_3]$ (Ln = Nd, **3**; Ln = Gd, **4**) were obtained by the further reaction with $\text{Ln}(\text{NO}_3)_3 \cdot 6\text{H}_2\text{O}$ (Ln = Nd or Gd). The result of their photophysical properties shows that the strong and characteristic near-infrared (NIR) luminescence of Nd^{3+} ions for complexes **1** and **3** with emissive lifetimes in microsecond range, has been sensitized from the excited state (^1LC and ^3LC) of the benzimidazole-based ligands, and the involvement of heavy atoms (Br) at the ligand endows the enhanced NIR luminescent property.

© 2012 Elsevier B.V. All rights reserved.

* Corresponding authors. Tel./fax: +86 29 88302312.

E-mail addresses: fwxdk@foxmail.com (W. Feng), lvxq@nwu.edu.cn (X. Lü).

Introduction

There is considerable interest in the near infrared (NIR) luminescent Nd^{3+} complexes due to their potential applications in bio-analysis [1] and materials science [2]. However, the f–f transitions for the Nd^{3+} ion are partially forbidden, the absorption coefficients and the emissive rates are very low [3]. In order to obtain efficient emissions, many organic (cyclic or acyclic) ligands [4] and d-block metal complexes [5] have been used as antennae or chromophores for the effective sensitization of NIR luminescence of the Nd^{3+} ion. Meanwhile, the role of suitable chromophores is to shield the Nd^{3+} ion against OH-, CH- or NH-oscillators in order to avoid or decrease luminescent quenching effect [6], and on the other hand, to allow the realization of the energy level's match of the excited state of the chromophore to the Nd^{3+} ion's exciting state [7].

Our past studies showed that in the formation of the series of Zn–Ln heterometallic complexes from the compartmental Salen-type Schiff-base ligands with the outer O_2O_2 moieties from MeO groups [8] or without [9], and the asymmetric Salen-type Schiff-base ligands with OH group [10], the Zn^{2+} complexes based on the Salen-type Schiff-base ligands, as the suitable chromophores, could effectively sensitize the NIR luminescence of the centered Ln^{3+} ions. Meanwhile, from the viewpoint of enhanced NIR luminescent properties, the use of the flexible linker while not the rigid one of the Salen-type Schiff-base ligands, could improve the NIR luminescent quantum efficiency due to the effective intramolecular energy transfer from the ligand-centered ^3LC and ^1LC not just ^1LC excited state to the Ln^{3+} ions. Moreover, the occupation of **Py** (pyridine) at the axial position of the Zn^{2+} ion, was helpful for the strong NIR luminescence, which should be resulted from the effective decrease of the luminescent quenching effect arising from OH-, CH- or NH-oscillators around the Ln^{3+} ion. Furthermore, the involvement of heavy atoms (Br) on the Salen-type Schiff-base ligand could help to increase the quantum yield for the triplet state formation and enhanced the NIR sensitization of the Ln^{3+} ions. As a matter of fact, the use of the Salen-type Schiff-base ligands should not be necessary to bind both Zn^{2+} and Ln^{3+} ions. Especially, the recent report of one magnetic $[\text{Cu}(\text{HL}^1)_2\text{Tb}(\text{NO}_3)_3]$ from the benzimidazole-based ligand H_2L^1 ($\text{H}_2\text{L}^1 = 2-(1\text{H-benzo[d]imidazol-2-yl})-6\text{-methoxyphenol}$) [11] stimulated us the further exploration on the possibility of its Zn^{2+} and Ln^{3+} luminescent complexes, despite much research on the luminescent Ln^{3+} complexes from the benzimidazole-based ligands [12]. Herein, with the compound $[\text{Zn}(\text{HL}^1)_2(\text{Py})]$ (**Py** = pyridine) or $[\text{Zn}(\text{HL}^2)_2(\text{Py})]$ ($\text{H}_2\text{L}^2 = 2-(1\text{H-benzo[d]imidazol-2-yl})-4\text{-bromo-6-methoxyphenol}$) as the precursor, complexes $[\text{ZnLn}(\text{HL}^1)_2(\text{Py})(\text{NO}_3)_3]$ ($\text{Ln} = \text{Nd}$, **1**; $\text{Ln} = \text{Gd}$, **2**) or $[\text{ZnLn}(\text{HL}^2)_2(\text{Py})(\text{NO}_3)_3]$ ($\text{Ln} = \text{Nd}$, **3**; $\text{Ln} = \text{Gd}$, **4**) were obtained by the further reaction with $\text{Ln}(\text{NO}_3)_3 \cdot 6\text{H}_2\text{O}$ ($\text{Ln} = \text{Nd}$ or Gd). The sensitization and energy transfer for the NIR luminescence of the Nd^{3+} ions in the two Zn–Nd complexes (**1** and **3**) were discussed.

Experimental section

Materials and methods

All chemicals were commercial products of reagent grade and were used without further purification. Elemental analyses were performed on a Perkin–Elmer 240C elemental analyzer. Infrared spectra were recorded on a Nicolet Magna-IR 550 spectrophotometer in the region $4000\text{--}400\text{ cm}^{-1}$ using KBr pellets. ^1H NMR spectra were recorded on a JEOL EX270 spectrometer with SiMe_4 as internal standard in CD_3CN at room temperature. ESI-MS was performed on a Finnigan LCQ^{DECA} XP HPLC–MS_n mass spectrometer with a mass to charge (m/z) range of 4000 using a standard electrospray ion source and CH_3CN as solvent. Electronic absorption spec-

tra in the UV/vis region were recorded with a Cary 300 UV spectrophotometer, and steady-state visible fluorescence, PL excitation spectra on a Photon Technology International (PTI) Alpha-scan spectrofluorometer and visible decay spectra on a pico-N₂ laser system (PTI Time Master). The quantum yield of the visible luminescence for each sample was determined by the relative comparison procedure, using a reference of a known quantum yield (quinine sulfate in dilute H_2SO_4 solution, $\Phi_{\text{em}} = 0.546$). NIR emission and excitation in solution were recorded by PTI QM4 spectrofluorometer with a PTI QM4 Near-Infrared InGaAs detector. The XRD patterns were recorded on a D/Max-III A diffractometer with graphite-monochromatized $\text{Cu K}\alpha$ radiation ($\lambda = 1.5418\text{ \AA}$). Thermogravimetric analyses were carried out on a NETZSCH TG 209 instrument under flowing nitrogen by heating the samples from 25 to $1000\text{ }^\circ\text{C}$.

Synthesis

2-(1H-benzo[d]imidazol-2-yl)-6-methoxyphenol (H_2L^1)

The ligand H_2L^1 was prepared according to the improved procedure from the literature [11]. A solution of *o*-vanillin (3.04 g, 20 mmol) in absolute EtOH (10 ml) was added slowly to the solution of *o*-phenylenediamine (2.16 g, 20 mmol) in absolute EtOH (10 ml) under a nitrogen atmosphere, and the resulting mixture was stirred overnight at room temperature. The insoluble orange precipitate was filtered off, and was added to absolute EtOH (20 ml) and then the mixture was refluxed for 12 h. After cooling to room temperature, the resulting off-white microcrystalline precipitate was filtered off, and washed with absolute EtOH and diethyl ether. Yield: 1.46 g, 61%. Calc. for $\text{C}_{14}\text{H}_{12}\text{N}_2\text{O}_2$: C, 69.99; H, 5.03; N, 11.66%; found: C, 69.91; H, 5.07; N, 11.65%. IR (KBr, cm^{-1}): 3337 (b), 1899 (w), 1836 (w), 1768 (w), 1625 (w), 1593 (w), 1532 (m), 1495 (s), 1475 (s), 1463 (s), 1450 (s), 1424 (s), 1391 (s), 1333 (m), 1304 (w), 1281 (m), 1262 (s), 1196 (w), 1181 (w), 1155 (w), 1088 (m), 1060 (s), 1009 (w), 981 (m), 954 (w), 930 (w), 909 (m), 863 (m), 831 (s), 788 (s), 745 (s), 717 (m), 651 (m), 633 (m), 603 (s), 571 (w), 555 (w), 520 (w), 501 (m), 440 (m), 419 (w). ^1H NMR (400 MHz, CD_3CN): δ (ppm) 13.42 (s, 1H, –NH), 13.27 (s, 1H, –OH), 7.67 (d, 1H, –Ph), 7.45 (m, 2H, –Ph), 7.32 (m, 2H, –Ph), 7.10 (d, 1H, –Ph), 6.93 (t, 1H, –Ph), 3.83 (s, 3H, –OMe).

The precursor of $[\text{Zn}(\text{HL}^1)_2(\text{Py})]$

To a stirred solution of H_2L^1 (240 mg, 1 mmol) in absolute EtOH (10 ml), solid $\text{Zn}(\text{OAc})_2 \cdot 2\text{H}_2\text{O}$ (110 mg, 0.5 mmol) and absolute pyridine (**Py**, 2 ml) were added separately, and the final mixture was heated under reflux for 5 h. After cooling to room temperature, the yellow insoluble precipitate was filtered out, washed with absolute EtOH and CHCl_3 , and dried under vacuum. For $[\text{Zn}(\text{HL}^1)_2(\text{Py})]$: yield: 230 mg, 74%. Calc. for $\text{C}_{33}\text{H}_{27}\text{N}_5\text{O}_4\text{Zn}$: C, 63.62; H, 4.37; N, 11.24%; found: C, 63.51; H, 4.43; N, 11.25%. IR (KBr, cm^{-1}): 3420 (w), 3058 (w), 2828 (w), 1625 (m), 1606 (m), 1536 (m), 1456 (vs), 1384 (w), 1349 (w), 1316 (m), 1292 (w), 1238 (s), 1203 (s), 1181 (m), 1164 (m), 1090 (m), 1070 (s), 1015 (w), 1000 (w), 933 (w), 912 (w), 852 (m), 781 (m), 733 (s), 665 (m), 632 (w), 562 (w), 507 (m), 434 (w). ^1H NMR (400 MHz, CD_3CN): δ (ppm) 13.33 (s, 2H, –NH), 8.58 (d, 2H, –Ph), 7.79 (t, 2H, –Ph), 7.60 (t, 4H, –Ph), 7.39 (m, 2H, –Ph), 7.24 (t, 2H, –Py), 7.04 (m, 3H, –Py), 6.91 (d, 2H, –Ph), 6.62 (t, 2H, –Ph), 3.68 (s, 6H, –OMe).

$[\text{ZnLn}(\text{HL}^1)_2(\text{Py})(\text{NO}_3)_3]$ ($\text{Ln} = \text{Nd}$, **1**; $\text{Ln} = \text{Gd}$, **2**)

To a stirred solution of $[\text{Zn}(\text{HL}^1)_2(\text{Py})]$ (0.063 g, 0.10 mmol) in absolute MeOH (5 ml), the solution of $\text{Ln}(\text{NO}_3)_3 \cdot 6\text{H}_2\text{O}$ (0.10 mmol, $\text{Ln} = \text{Nd}$, 0.043 g; $\text{Ln} = \text{Gd}$, 0.044 g) in absolute acetone (4 ml) were added, sequentially, and the mixture was reflux for about 3 h. The respective yellow clear solution was then cooled to room temperature and filtered. Diethyl ether was allowed to diffuse slowly into

the respective solution at room temperature and pale yellow microcrystallines **1–2** were obtained in about three weeks, respectively. For **1**: Yield: 0.065 g, 68%. Calc. for $C_{33}H_{27}N_8O_{13}ZnNd$: C, 41.58; H, 2.85; N, 11.75%; found: C, 41.69; H, 2.91; N, 11.76%. IR (KBr, cm^{-1}): 3270 (w), 2336 (w), 2103 (w), 1895 (w), 1769 (w), 1652 (m), 1625 (m), 1609 (m), 1571 (m), 1540 (m), 1453 (vs), 1385 (s), 1318 (s), 1303 (s), 1201 (m), 1180 (m), 1162 (m), 1120 (w), 1092 (m), 1055 (s), 991 (m), 931 (w), 909 (w), 863 (m), 846 (m), 817 (w), 782 (m), 744 (s), 703 (m), 658 (m), 630 (w), 561 (w), 539 (w), 508 (m), 442 (m), 420 (m). 1H NMR (400 MHz, CD_3CN): δ (ppm) 14.59 (s, 2H), 9.40 (d, 2H), 8.61 (m, 2H), 7.72 (m, 4H), 7.61 (m, 2H), 7.48 (m, 2H), 6.92 (m, 3H), 6.46 (m, 2H), 5.72 (m, 2H), -2.65 (s, 6H). ESI-MS (CH_3CN) m/z : 950.01 ($[M-H]^+$, 100%). For **2**: Yield: 0.060 g, 62%. Calc. for $C_{33}H_{27}N_8O_{13}ZnGd$: C, 41.02; H, 2.82; N, 11.60%; found: C, 40.98; H, 2.86; N, 11.58%. IR (KBr, cm^{-1}): 3427 (w), 2318 (w), 2041 (w), 1967 (w), 1765 (w), 1637 (m), 1616 (m), 1585 (m), 1571 (m), 1551 (m), 1522 (m), 1457 (vs), 1387 (s), 1330 (s), 1303 (s), 1286 (m), 1263 (m), 1234 (m), 1195 (m), 1167 (m), 1120 (w), 1096 (m), 1074 (m), 1023 (m), 966 (m), 850 (m), 815 (w), 784 (m), 740 (s), 666 (m), 648 (w), 632 (w), 582 (w), 556 (w), 540 (w), 512 (m), 442 (m), 415 (m). ESI-MS (CH_3CN) m/z : 966.03 ($[M-H]^+$, 100%).

2-(1H-benzodimidazol-2-yl)-4-bromo-6-methoxyphenol (H_2L^2)

The benzimidazole-based ligand H_2L^2 was prepared in the same way as that of H_2L^1 except *o*-phenylenediamine (2.16 g, 20 mmol) and 5-bromo-2-hydroxy-3-methoxybenzaldehyde (4.62 g, 20 mmol) were used. The off-white microcrystalline precipitate was obtained by washing with absolute EtOH and diethyl ether. Yield: 1.62 g, 70%. Calc. for $C_{14}H_{11}BrN_2O_2$: C, 52.69; H, 3.47; N, 8.78%; found: C, 52.66; H, 3.49; N, 8.77%. IR (KBr, cm^{-1}): IR (KBr, cm^{-1}): 3934 (w), 3362 (w), 2473 (w), 2344 (w), 1922 (w), 1628 (m), 1464 (m), 1444 (m), 1385 (m), 1327 (s), 1249 (vs), 1114 (m), 983 (s), 911 (m), 825 (vs), 735 (vs), 708 (vs), 601 (v), 548 (w). 1H NMR (400 MHz, CD_3CN): δ 13.65 (s, H, -NH), 13.40 (s, 1H, -OH), 7.63 (d, 1H, -Ph), 7.49 (d, 1H, -Ph), 7.37 (m, 1H, -Ph), 7.31 (m, 1H, -Ph), 7.12 (m, 2H, -Ph), 3.93 (s, 3H, -MeO).

The precursor of $[Zn(HL^2)_2(Py)]$

The method was similar to that used for $[Zn(HL^1)_2(Py)]$ (above). H_2L^2 (319 mg, 1 mmol), $Zn(OAc)_2 \cdot 2H_2O$ (110 mg, 0.5 mmol) and Py (2 ml) were employed. Finally, the yellow precipitate was filtered out, washed with absolute EtOH and $CHCl_3$, and dried under vacuum. For $[Zn(HL^2)_2(Py)]$: yield: 245 mg, 70%. Calc. for $C_{33}H_{25}Br_2N_8O_{13}Zn$: C, 50.76; H, 3.23; N, 8.97%; found: C, 50.70; H, 3.31; N, 8.98%. IR (KBr, cm^{-1}): 3436 (w), 3184 (w), 2930 (w), 2343 (w), 2119 (w), 1626 (m), 1530 (s), 1471 (m), 1382 (w), 1313 (s), 1232 (vs), 1179 (m), 1069 (s), 1000 (w), 887 (m), 841 (m), 799 (vs), 740 (vs), 634 (m), 567 (m), 508 (s), 419 (s). 1H NMR (400 MHz, CD_3CN): δ 13.49 (s, 2H, -NH), 8.57 (s, 1H, -Ph), 7.82 (s, 2H, -Ph), 7.58 (d, 2H, -Ph), 7.39 (t, 2H, -Ph), 7.26 (t, 2H, -Ph), 7.14 (t, 2H, -Ph), 7.09 (m, 4H, -Ph), 6.98 (s, 2H, -Ph), 3.70 (s, 6H, -MeO).

$[ZnLn(HL^2)_2(Py)(NO_3)_3]$ ($Ln = Nd$, **3**; $Ln = Gd$, **4**)

To a stirred solution of $[Zn(HL^2)_2(Py)]$ (0.078 g, 0.10 mmol) in absolute MeCN (5 ml), the solution of $Ln(NO_3)_3 \cdot 6H_2O$ (0.10 mmol, $Ln = Nd$, 0.043 g or $Ln = Gd$, 0.044 g) in absolute acetone (4 ml) was added, and the mixture was refluxed about 3 h. The respective yellow clear solution was then cooled to room temperature and filtered. Diethyl ether was allowed to diffuse slowly into the respective solution at room temperature and pale yellow microcrystallines **3** or **4** was obtained after three weeks, respectively. For **3**: Yield: 0.080 g, 71%. Calc. for $C_{33}H_{25}Br_2N_8O_{13}ZnNd$: C, 35.67; H, 2.27; N, 10.09%; found: C, 35.72; H, 2.33; N, 10.08%. IR (KBr, cm^{-1}): 3310 (w), 3090 (w), 2935 (w), 2114 (w), 1935 (w), 1595 (m), 1474 (w), 1457 (s), 1385 (m), 1314 (s), 1248 (s),

1179 (m), 1059 (m), 986 (s), 847 (m), 798 (s), 766 (vs), 703 (s), 634 (m), 566 (m), 507 (s), 454 (m). 1H NMR (400 MHz, CD_3CN): δ 14.71 (s, 2H, -NH), 9.42 (s, 1H, -Ph), 8.62 (s, 2H, -Ph), 7.75 (d, 2H, -Ph), 7.60 (t, 2H, -Ph), 7.49 (t, 2H, -Ph), 7.10 (t, 2H, -Ph), 6.42 (m, 4H, -Ph), 5.67 (s, 2H, -Ph), -3.14 (s, 6H, -MeO). ESI-MS (CH_3CN) m/z : 1105.84 ($[M-H]^+$, 100%). For **4**: Yield: 0.055 g, 62%. Calc. for $C_{33}H_{25}Br_2N_8O_{13}ZnGd$: C, 35.26; H, 2.24; N, 9.97%; found: C, 35.25; H, 2.31; N, 9.91%. IR (KBr, cm^{-1}): 3316 (w), 3090 (w), 2932 (w), 2110 (w), 1936 (w), 1594 (m), 1480 (w), 1451 (s), 1385 (m), 1317 (m), 1248 (s), 1179 (m), 1060 (m), 986 (s), 847 (m), 799 (vs), 746 (vs), 703 (vs), 634 (m), 545 (m), 508 (s), 452 (m). ESI-MS (CH_3CN) m/z : 1121.85 ($[M-H]^+$, 100%).

X-ray crystallography

Single crystals of **1**·1.5MeOH·1.5H₂O·0.5Py and **3**·Py of suitable dimensions were mounted onto thin glass fibers. All the intensity data were collected on a Bruker SMART CCD diffractometer (Cu-K α radiation and $\lambda = 1.54184 \text{ \AA}$ for **1**·1.5MeOH·1.5H₂O·0.5Py; Mo-K α radiation and $\lambda = 0.71073 \text{ \AA}$ for **3**·Py) in ϕ and ω scan modes. Structures were solved by direct methods followed by difference Fourier syntheses, and then refined by full-matrix least-squares techniques against F^2 using SHELXTL [13]. All other non-hydrogen atoms were refined with anisotropic thermal parameters. Absorption corrections were applied using SADABS [14]. All hydrogen atoms were placed in calculated positions and refined isotropically using a riding model. Crystallographic data and refinement parameters for the complexes are presented in Table 1. Relevant atomic distances and bond angles are collected in Table 2.

Results and discussion

Synthesis and characterization

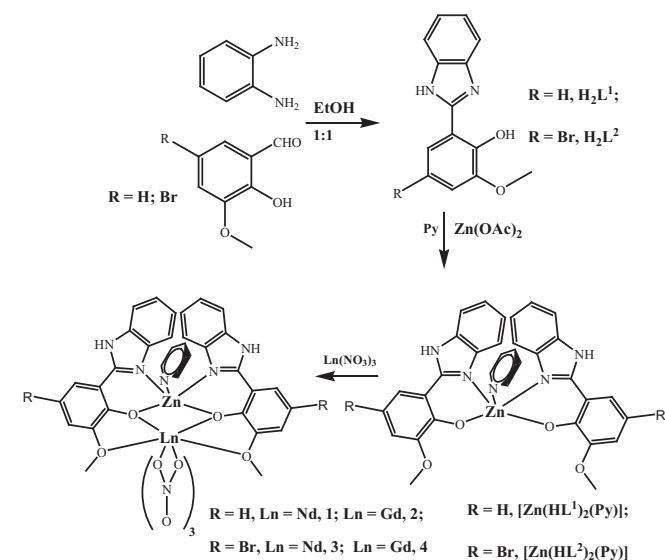
As shown in Scheme 1, treatment of *o*-phenylenediamine with *o*-vanillin or 5-bromo-2-hydroxy-3-methoxybenzaldehyde in 1:1 molar ratio in absolute EtOH at ambient temperature and the sub-

Table 1
Crystallographic data and refinement parameters for complexes **1**·1.5MeOH·1.5H₂O·0.5Py and **3**·Py.

Compound	1 ·1.5MeOH·1.5H ₂ O·0.5Py	3 ·Py
Empirical formula	$C_{37}H_{38.5}N_{8.5}O_{16}ZnNd$	$C_{38}H_{30}N_9O_{13}Br_2ZnNd$
Formula weight	1067.87	1090.14
Crystal system	Triclinic	Triclinic
Space group	<i>P</i> -1	<i>P</i> -1
$\lambda/\text{\AA}$	1.54184	0.71073
<i>a</i> / \AA	11.4753(6)	11.407(4)
<i>b</i> / \AA	15.6752(9)	14.335(5)
<i>c</i> / \AA	26.4003(16)	15.257(6)
$\alpha/^\circ$	93.742(5)	106.740(7)
$\beta/^\circ$	90.597(5)	103.261(7)
$\gamma/^\circ$	106.176(5)	91.570(7)
$V/\text{\AA}^3$	4549.1(4)	2313.7(15)
<i>Z</i>	4	2
$\rho/g\text{ cm}^{-3}$	1.559	1.708
Crystal size/mm	$0.31 \times 0.27 \times 0.23$	$0.28 \times 0.26 \times 0.22$
μ/mm^{-1}	9.916	3.424
Data/restraints/parameters	8748/0/1144	8139/0/548
Quality-of-fit indicator	1.020	0.970
No. Unique reflections	8748	8139
No. Observed reflections	10321	11489
Final <i>R</i> indices [$I > 2\sigma(I)$]	$R_1 = 0.0863$ $wR_2 = 0.2289$	$R_1 = 0.0975$ $wR_2 = 0.2227$
<i>R</i> indices (all data)	$R_1 = 0.1015$ $wR_2 = 0.2484$	$R_1 = 0.2289$ $wR_2 = 0.3097$

Table 2
Selected interatomic distances/Å and bond angles/° with esds for complexes **1**·1.5MeOH·1.5H₂O·0.5Py and **3**·Py.

1·1.5MeOH·1.5H ₂ O·0.5Py		3·Py	
Zn(1)–N(1) 2.053(14)	Nd(1)–O(1) 2.549(9)	Zn(1)–N(1) 2.006(16)	
Zn(1)–N(3) 2.026(14)	Nd(1)–O(2) 2.421(9)	Zn(1)–N(3) 2.004(15)	
Zn(1)–N(5) 2.083(12)	Nd(1)–O(3) 2.354(9)	Zn(1)–N(5) 2.124(16)	
Zn(1)–O(2) 2.042(8)	Nd(1)–O(4) 2.667(9)	Zn(1)–O(2) 2.061(11)	
Zn(1)–O(3) 2.117(11)	Nd(1)–O(5) 2.561(11)	Zn(1)–O(3) 2.100(13)	
	Nd(1)–O(7) 2.603(10)		
Zn(2)–N(9) 2.060(10)	Nd(1)–O(8) 2.504(10)	Nd(1)–O(1) 2.641(12)	
Zn(2)–N(11) 2.019(12)	Nd(1)–O(10) 2.609(10)	Nd(1)–O(2) 2.488(11)	
	Nd(1)–O(11) 2.512(11)		
Zn(2)–N(13) 2.110(12)	Nd(1)–O(13) 2.468(11)	Nd(1)–O(3) 2.380(12)	
Zn(2)–O(15) 2.041(9)		Nd(1)–O(4) 2.780(13)	
Zn(2)–O(16) 2.101(8)		Nd(1)–O(5) 2.561(15)	
	Nd(2)–O(14) 2.563(9)	Nd(1)–O(7) 2.528(12)	
N(1)–Zn(1)–N(3) 101.1(5)	Nd(1)–O(15) 2.434(8)	Nd(1)–O(8) 2.617(14)	
N(1)–Zn(1)–N(5) 93.2(5)	Nd(1)–O(16) 2.374(9)	Nd(1)–O(10) 2.575(16)	
N(1)–Zn(1)–O(2) 88.4(4)	Nd(1)–O(17) 2.692(9)	Nd(1)–O(11) 2.571(15)	
N(1)–Zn(1)–O(3) 162.6(4)	Nd(1)–O(18) 2.571(11)	Nd(1)–O(13) 2.540(14)	
	Nd(1)–O(20) 2.626(9)		
N(9)–Zn(2)–N(11) 105.9(4)	Nd(1)–O(21) 2.517(9)	N(1)–Zn(1)–N(3) 107.3(7)	
N(9)–Zn(2)–N(13) 95.9(5)	Nd(1)–O(23) 2.604(9)	N(1)–Zn(1)–N(5) 94.7(6)	
		N(1)–Zn(1)–O(2) 87.9(6)	
N(9)–Zn(2)–O(15) 87.1(4)	Nd(1)–O(24) 2.512(10)	N(1)–Zn(1)–O(3) 164.3(6)	
N(9)–Zn(2)–O(16) 162.4(4)	Nd(1)–O(26) 2.465(10)		



Scheme 1. Syntheses of the ligands, the precursors and the series of hetero-binuclear Zn–Ln complexes **1–4**.

sequent refluxing in absolute EtOH, produced the off-white benzimidazole-based ligand **H₂L¹** or **H₂L²** in the good yield, respectively. Reaction of the benzimidazole-based ligand **H₂L¹** or **H₂L²** and Zn(OAc)₂·2H₂O in 2:1 molar ratio in the presence of excess absolute pyridine (Py) afforded the respective precursor [Zn(HL¹)₂(Py)] or [Zn(HL²)₂(Py)] in good yield of ca. 70%. Further reaction the precursor [Zn(HL¹)₂(Py)] or [Zn(HL²)₂(Py)] with the Ln(NO₃)₃·6H₂O (Ln = Nd or Gd) resulted in the formation of two series of the hetero-binuclear Zn–Ln complexes [Zn(HL¹)₂(Py)]Ln(NO₃)₃ (Ln = Nd, **1** or Ln = Gd, **2**), or [Zn(HL²)₂(Py)]Ln(NO₃)₃ (Ln = Nd, **3** or Ln = Gd, **4**), respectively. For complexes **1** and **3**, Sin-

gle crystal of **1**·1.5MeOH·1.5H₂O·0.5Py or **3**·Py suitable for X-ray diffraction studies was obtained by allowing Et₂O to diffuse into the respective mixture (MeOH–Py) at room temperature.

The IR spectra of complexes **1–4** show two strong absorptions at 1451–1457 and 1314–1320 cm⁻¹, which are typical for the bidentate NO₃⁻ groups, and the bands appearing at 766 or 758 cm⁻¹ assigned as the ν(C–Br) vibration in complex **3** or **4**, respectively. The ¹H NMR spectrum identification of **H₂L¹** or **H₂L²** in CD₃CN with a sharp singlet at δ = 13.27 ppm or 13.40 ppm for the –OH proton, exhibits the typical resonance-assisted hydrogen bonded (RAHB) proton of the type O–H···N [15]. As to the room temperature ¹H NMR spectrum of complex **1** or **3** in CD₃CN, one set of the proton resonances of the (HL¹)⁻ or (HL²)⁻ ligand while with large shifts (δ from 14.59 to –2.65 ppm for **1** and δ from 14.71 to –3.14 ppm for **3**) are observed, due to the Nd³⁺-induced shift, significantly spread in relative to those of the free ligand (δ from 13.42 to 3.83 ppm for **H₂L¹** or δ from 13.65 to 3.93 ppm for **H₂L²**) and the precursor (δ from 13.33 to 3.68 ppm for [Zn(HL¹)₂(Py)] or δ from 13.49 to 3.70 ppm) for [Zn(HL²)₂(Py)]. The ESI-MS spectra of the four Zn–Ln complexes (**1–4**) exhibit the strongest peak at *m/z* 950.00 (**1**), 966.03 (**2**), 1105.84 (**3**) or 1121.85 (**4**), respectively, corresponding to the major species [ZnLn(HL¹)₂(Py)(NO₃)₃] (Ln = Nd, **1**; Ln = Gd, **2**) or [ZnLn(HL²)₂(Py)(NO₃)₃] (Ln = Nd, **3**; Ln = Gd, **4**), further indicating that the discrete Zn–Ln (Ln = Nd or Gd) molecule exists in the respective dilute MeCN solution. Thermogravimetric analysis (TGA) of the four polycrystalline complexes shows the similar weight loss patterns, as shown in Figs. 1s and 2s, respectively. The gradual weight loss (ca. 10% for **1**·1.5MeOH·1.5H₂O·0.5Py or **2**·1.5MeOH·1.5H₂O·0.5Py and ca. 7% for **3**·Py or **4**·Py) occurred between 25 and 210 or 180 °C, indicative of the loss of the respective solvated molecules, and the frameworks decomposed at ca. 308 or 315 °C with an observed abrupt weight loss.

Structures of Complexes **1** and **3**

X-ray quality crystals of **1**·1.5MeOH·1.5H₂O·0.5Py as the representative of the two Zn–Ln complexes based on the **H₂L¹** ligand were obtained, and the tables of selected crystal properties are given in Tables 1 and 2. Complex **1**·1.5MeOH·1.5H₂O·0.5Py crystallizes with two independent hetero-binuclear molecules and solvates of MeOH, H₂O and Py in the asymmetrical unit shown in Fig. 3s. As shown in Fig. 1, in both Zn–Nd molecules, two deprotonated (HL¹)⁻ ligands sandwich one Zn²⁺ ion through their N,O sites and one Nd³⁺ ion through their O₂ site, endowing a relative arrangement close to head-to-head. Each Zn²⁺ (Zn1 or Zn2) ion has a five-coordinate environment and adopts a distorted square pyramidal geometry, composed of the inner N₂O₂ core from two deprotonated benzimidazole-based (HL¹)⁻ ligands as the base plane, and one N atom from the coordinated Py at the apical position. The Nd³⁺ ion in both Zn–Nd molecules is bridged the respective Zn²⁺ ion by two phenoxo oxygen atoms of two (HL¹)⁻ ligands with the similar Zn···Nd separation of 3.636(3) Å. Each Nd³⁺ ion is ten-coordinate. In addition to the four oxygen atoms from two deprotonated benzimidazole-based (HL¹)⁻ ligands, they complete their coordination environments with six oxygen atoms from three bidentate NO₃⁻ anions. The lengths (2.026(14)–2.053(14) or 2.019(12)–2.060(10) Å) of Zn–N (the benzimidazole (HL¹)⁻ ligands, N1 and N3 or N11 and N13) bonds are smaller than that (2.083(12) or 2.110(12) Å) of Zn–N (Py, N5 or N15) bond while between those (2.042(8)–2.117(11) or 2.041(9)–2.101(8) Å) of Zn–O (phenoxo, O2 and O3 or O15 and O16) bonds. The Nd–O bond lengths depend on the nature of the oxygen atoms: they vary from 2.354(9)–2.667(9) Å, and the bond lengths from oxygen atoms of NO₃⁻ anions are longer than those from phenoxo oxygen atoms, while slightly shorter than those from –OMe groups. Moreover, the large dihedral angles (14.8(3)° and 23.9(3)° or 20.7(3)° and 23.2(3)°) in

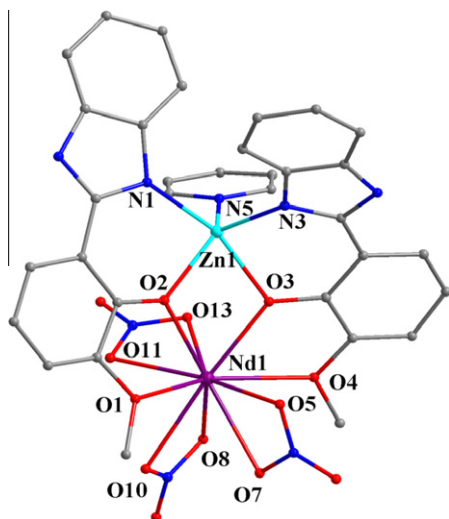


Fig. 1. Perspective drawing of one of the hetero-binuclear part in complex **1**·1.5MeOH·1.5H₂O·0.5Py, H atoms, the other hetero-binuclear part and solvates are omitted for clarity.

both Zn–Nd molecules between the benzimidazole moieties and the substituted aryl rings, should be due to the coordination of metal ions. Besides the inter-molecular N10–H10···N17 hydrogen bonding with the N···N distance of 2.850(2) Å between the solvate **Py** and one of the Zn–Nd molecules, as shown in Fig. 3s, the other solvate molecules (MeOH or H₂O) are not bound to the framework and they exhibit no observable interactions with the host structure.

The involvement of heavy atoms (Br) did not lead to a significant change of the hetero-binuclear Zn–Ln structures from the replacement of the benzimidazole-based ligand **H₂L²**. X-ray quality crystals of **3**·Py as the representative of the two Zn–Ln complexes based on the **H₂L²** ligand were obtained, and the tables of selected crystal properties are also given in Tables 1 and 2. Complex **3**·Py crystallizes with one independent hetero-binuclear molecule and one solvate of **Py** in the asymmetrical unit, as shown in Fig. 2. The slightly shorter Zn–N (benzimidazole) bond lengths (2.004(15)–2.006(16) Å) and the slightly longer Zn···Nd separation (3.688(3) Å) in complex **3**·Py than those of complex **1**·1.5 MeOH·1.5H₂O·0.5Py, respectively, should be resulted from the with-drawing electronic effect of Br atoms with the use of the benzimidazole-based ligand **H₂L²**. The inter-molecular N4–H4···N9 hydrogen bonding with N···N distance of 2.769(3) Å

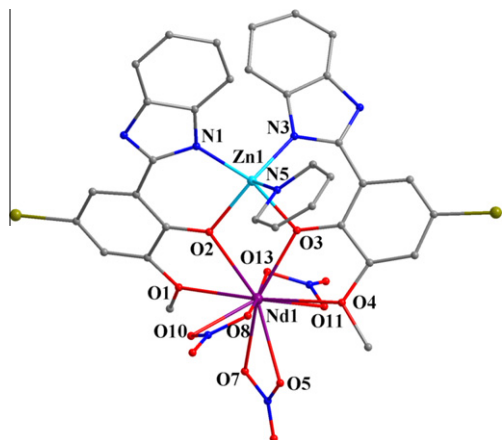


Fig. 2. Perspective drawing of complex **3**·Py, H atoms and solvates are omitted for clarity.

between the solvate **Py** and the Zn–Nd molecule, as shown in Fig. 4s, is also observed. It is worth noting that in the formation of two Zn–Nd arrayed complexes **1**·1.5MeOH·1.5H₂O·0.5Py and **3**·Py, incomparable of that of magnetic [Cu(HL¹)₂Tb(NO₃)₃] [11] where the Cu²⁺ ion is four-coordinate and has a square-planar geometry, the occupation of **Py** at the axial position of Zn²⁺ ions is considered to completely avoid the further coordination of solvents around the Nd³⁺ ions of the two Zn–Nd complexes. As to the bulk purity of the polycrystalline complexes **1**·1.5MeOH·1.5H₂O·0.5Py and **3**·Py, it is convincingly established by X-ray powder diffraction measurements. As shown in Figs. 5s and 6s, respectively, for each of the two complexes, the peak positions of the measured pattern closely match those of the respective simulated **1**·1.5MeOH·1.5H₂O·0.5Py or **3**·Py, confirming that a single phase is formed for each complex.

Photophysical properties

The photophysical properties of the precursor [Zn(HL¹)₂(Py)] or [Zn(HL²)₂(Py)] and complexes **1–4** have been examined in dilute MeCN solution at room temperature or 77 K, and summarized in Table 3 and Figs. 3–7. As shown in Fig. 3, the similar ligand-centered solution absorption spectra (225–230, 298–301 and 339–340 nm) of complexes **1–2** to that (226, 301 and 358 nm) of the precursor [Zn(HL¹)₂(Py)] in the UV–vis region are observed, while the lowest energy absorptions of complexes **1–2** are blue-shifted by 18–19 nm upon the further coordination of Ln³⁺ ions. For complex **1**, the residual visible emission band (ca. 503 nm and $\tau < 1$ ns, almost undetectable) and the low quantum yield ($\phi_{em} < 10^{-5}$) in dilute absolute MeCN solution at room temperature are observed, but photo excitation of the antenna in the range of 275–500 nm ($\lambda_{ex} = 377$ nm), as shown in Fig. 4, gives rise to the characteristic emissions of the Nd³⁺ ion ($^4F_{3/2} \rightarrow ^4I_{j/2}$, $J = 9, 11, 13$) in the NIR region: The emissions at 907, 1085 and 1354 nm can be assigned to $^4F_{3/2} \rightarrow ^4I_{9/2}$, $^4F_{3/2} \rightarrow ^4I_{11/2}$ and $^4F_{3/2} \rightarrow ^4I_{13/2}$ transitions of the Nd³⁺ ion, respectively. The precursor [Zn(HL¹)₂(Py)] or the complex **2** does not exhibit the NIR luminescence under the same condition, just has the typically strong luminescence ($\lambda_{em} = 528$ nm, $\tau = 1.37$ ns and $\phi = 14.3 \times 10^{-3}$ for the precursor [Zn(HL¹)₂(Py)]) or the weakened ($\lambda_{em} = 503$ nm, $\tau = 0.52$ ns and $\phi = 0.11 \times 10^{-3}$ for **2**) of the benzimidazole-based ligand **H₂L¹** in the visible region, as shown in Fig. 5. It is worth noting that for complex **1**, the similar excitation spectrum monitored at the NIR emission peak ($\lambda_{em} = 1085$ nm) to that of complex **2** at the weakened visible emission peak ($\lambda_{em} = 503$ nm), clearly showing both the visible and NIR emissions are originated from the same π – π^* transitions of the benzimidazole-based ligand **H₂L¹**, suggests that the energy transfer from the antenna to the Ln³⁺ ions takes place efficiently [16]. Moreover, for complex **1**, the luminescent decay curves obtained from time-resolved luminescent experiments can be fitted mono-exponentially with time constant of microseconds (1.26 μ s at 907 nm and 1.28 μ s at 1085 nm), and the intrinsic quantum yield ϕ_{Nd} (ca. 0.51%) of the Nd³⁺ emission may be estimated by $\phi_{Nd} = \tau_{obs}/\tau_0$, where τ_{obs} is the observed emission lifetime and τ_0 is the “natural lifetime”, viz 0.25 ms for the Nd³⁺ ion [17], which indicates the presence of single emitting center for complex **1** in dilute MeCN solutions [18]. Due to the limitation of our instrument, we were unable to determine the τ_{obs} value at 1354 nm for Nd³⁺ ion.

As a reference compound, complex **2** allows the further study of the antenna luminescence in the absence of energy transfer, because the Gd³⁺ ion has no energy levels below 32000 cm⁻¹, and therefore cannot accept any energy from the antennae excited state [19]. In dilute MeCN solution at 77 K, complex **2** displays the stronger antennae fluorescence than that ($\lambda_{em} = 503$ nm, $\tau = 0.52$ ns and $\phi = 0.11 \times 10^{-3}$) at room temperature on the same condition, which shows the higher luminescent intensity

Table 3
The photophysical properties of the precursors $[\text{Zn}(\text{HL}^1)_2(\text{Py})]$, $[\text{Zn}(\text{HL}^2)_2(\text{Py})]$ and complexes **1–4** at 2×10^{-5} M in absolute MeCN solution at room temperature or 77 K.

Compound	Absorption $\lambda_{\text{ab}}/\text{nm}$ [$\log(\epsilon/\text{dm}^3 \text{ mol}^{-1} \text{ cm}^{-1})$]	Excitation $\lambda_{\text{ex}}/\text{nm}$	Emission $\lambda_{\text{em}}/\text{nm}$ (τ , $\Phi \times 10^3$)
$[\text{Zn}(\text{HL}^1)_2(\text{Py})]$	226(0.38), 301(0.22), 358(0.11)	422	528(s, 1.37 ns, 14.3)
1	225(0.47), 298(0.28), 340(0.24)	377	503(w), 907(m, 1.26 μs), 1085(s, 1.28 μs), 1354 ^a
2	230(0.30), 301(0.32), 339(0.24)	385	503(m, 0.52 ns, 0.11)
$[\text{Zn}(\text{HL}^2)_2(\text{Py})]$	232(0.53), 303(0.039)	331, 451	486(s, 1.13 ns, 77 K), 535(s, 2.24 ms, 77 K)
3	243(0.54), 300(0.48), 341(0.42)	411	541(s, 1.81 ns, 19.4)
4	242(0.54), 301(0.48), 343(0.41)	414	511(w), 902(m, 1.54 μs), 1082(s, 1.57 μs), 1352 ^a
			512(m, 0.85 ns, 0.20)
			495(s, 1.44 ns, 77 K), 544(s, 3.41 ms, 77 K)

^a Due to the limitations of the instrument, we were unable to measure the lifetime of the NIR luminescence at 1300 nm above.

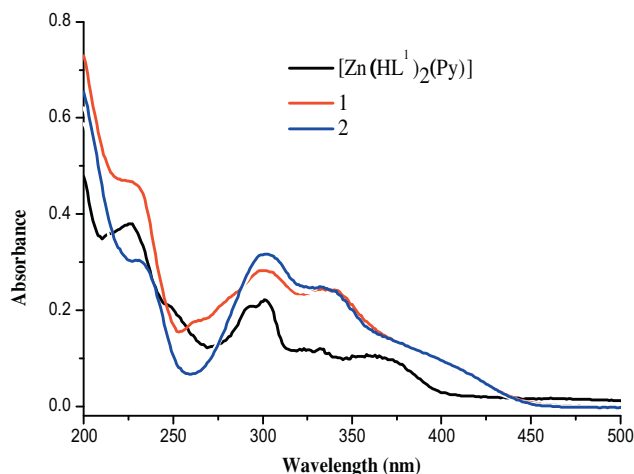


Fig. 3. UV-vis spectra of precursor $[\text{Zn}(\text{HL}^1)_2(\text{Py})]$ and complexes **1–2** in MeCN solution at 2×10^{-5} M at room temperature.

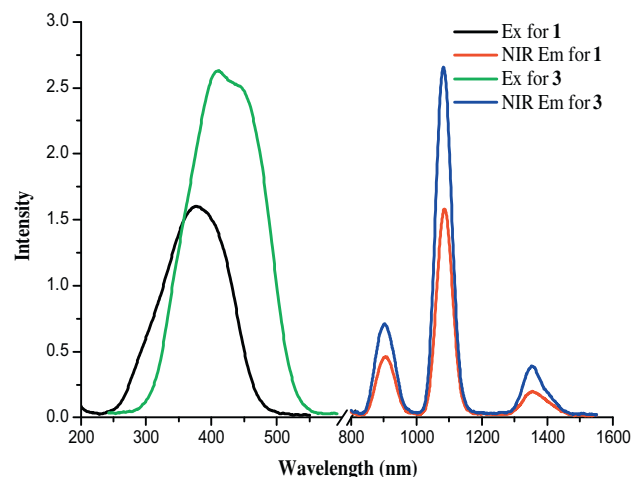


Fig. 4. NIR emission and excitation spectra of complexes **1** and **3** in MeCN solution at 2×10^{-5} M at room temperature.

($\lambda_{\text{em}} = 486$ and 535 nm) and the distinctively longer luminescence lifetimes (1.13 ns and 2.24 ms). This result shows that the sensitization of the NIR luminescence for complex **1** should arise from both the ^1LC (20576 cm^{-1}) and the ^3LC (18692 cm^{-1}) excited state of the benzimidazole-based ligand H_2L^1 at low temperature. If the antennae luminescence lifetime of complex **2** is to represent the excited-state lifetime in the absence of the energy transfer, the energy transfer rate (k_{ET}) in the complex **1** can thus be calculated from $k_{\text{ET}} = 1/\tau_{\text{q}} - 1/\tau_{\text{u}}$ [20], where τ_{q} is the residual lifetime of

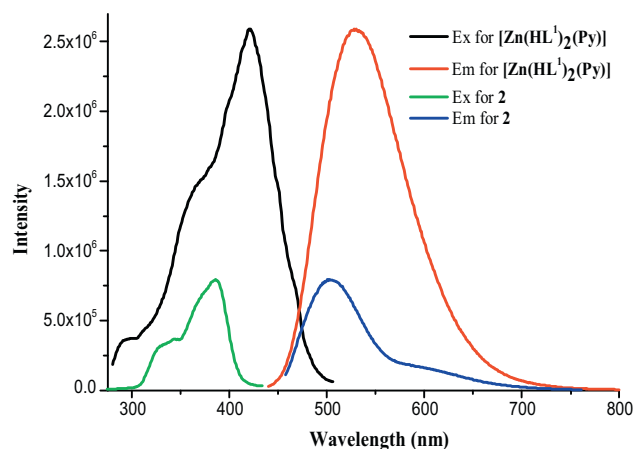


Fig. 5. Visible emission and excitation spectra of precursor $[\text{Zn}(\text{HL}^1)_2(\text{Py})]$ and complex **2** in MeCN solution at 2×10^{-5} M at room temperature.

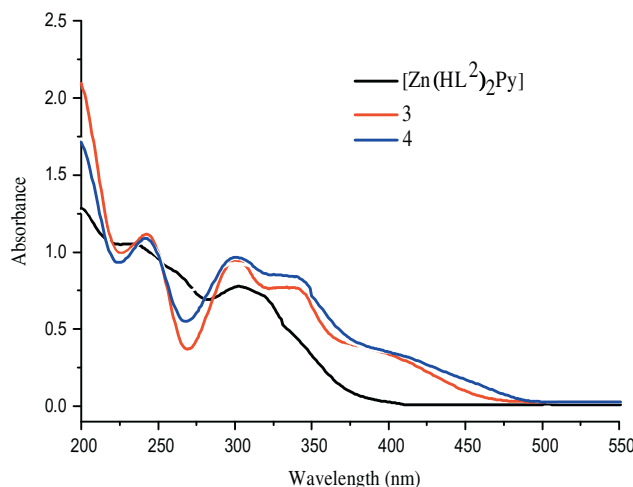


Fig. 6. UV-vis spectra of precursor $[\text{Zn}(\text{HL}^2)_2(\text{Py})]$ and complexes **3–4** in MeCN solution at 2×10^{-5} M at room temperature.

the Zn^{2+} -based emission undergoing quenching by the respective Ln^{3+} ion, and τ_{u} is the weakened while unquenched lifetime in the reference complex **2**, so the energy transfer rates for the Nd^{3+} ion in complex **1** may all be estimated to be above $5 \times 10^8 \text{ s}^{-1}$, which could well imply the reason to the effective energy transfer for complex **1**.

By extension of the conjugation through the involvement of heavy atoms (Br) from H_2L^1 to H_2L^2 , as shown in Table 3 and Fig. 6, the absorption spectra of the precursor $[\text{Zn}(\text{HL}^2)_2(\text{Py})]$ and

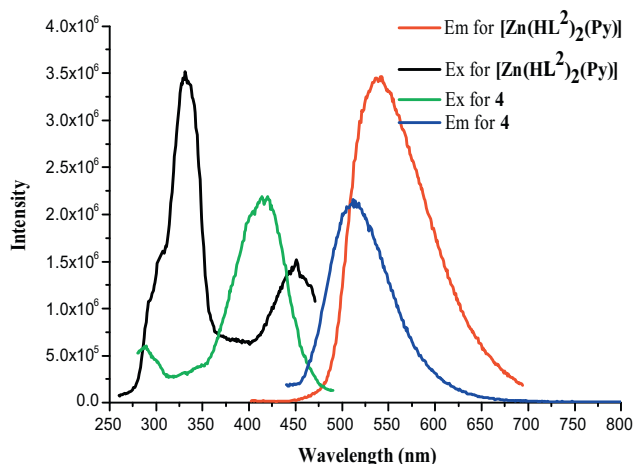


Fig. 7. Visible emission and excitation spectra of precursor $[\text{Zn}(\text{HL}^2)_2(\text{Py})]$ and complex **4** in MeCN solution at 2×10^{-5} M at room temperature.

complexes **3–4** are all red-shifted relative to those of the precursor $[\text{Zn}(\text{HL}^1)_2(\text{Py})]$ and complexes **1–2**, respectively. Moreover, for the precursor $[\text{Zn}(\text{HL}^2)_2(\text{Py})]$, the red-shifted emission maximum ($\lambda_{\text{em}} = 541$ nm, shown in Fig. 7) by about 13 nm, and the slightly higher quantum yield ($\phi = 19.4 \times 10^{-3}$) than those of the corresponding precursor $[\text{Zn}(\text{HL}^1)_2(\text{Py})]$ are observed, respectively. Similarly, for complex **3** in dilute MeCN solution at room temperature, the almost quenched visible emission ($\lambda_{\text{em}} = 511$ nm) and the strong characteristic NIR emissions of the Nd^{3+} ion ($^4\text{F}_{3/2} \rightarrow ^4\text{I}_{1/2}$, $J = 9, 11, 13$), as shown in Fig. 4, also suggest that the effective sensitization from the antenna of $(\text{HL}^2)^-$ ligands to the Nd^{3+} ion takes place [16]. Through the further investigation on the emission of the reference complex **4**, especially at 77 K, the strong antennae fluorescence ($\lambda_{\text{em}} = 495$ and 544 nm) and two luminescence lifetimes (1.44 ns and 3.41 ms) show that the sensitization of the NIR luminescence for complex **3** should also arise from both the ^1LC (20202 cm^{-1}) and the ^3LC (18382 cm^{-1}) excited state of the benzimidazole-based ligand H_2L^2 at low temperature.

We were naturally interested in the effect of heavy atom (Br) on the NIR luminescent property of the two Zn–Nd complexes **1** and **3**. Although there was almost no position shift of the NIR emissions of Nd^{3+} ions in solution at room temperature, each of the emission intensities of complex **3** was distinctively higher than the respective one of complex **1**, which is probably the result of the promotion of $^1\text{LC} \rightarrow ^3\text{LC}$ intersystem crossing by the involvement of heavy atoms [21]. On the other hand, for complex **3**, the longer lifetimes (1.54 μs at 902 nm and 1.57 μs at 1082 nm) and the larger intrinsic quantum yield ϕ_{Nd} (ca. 0.62%) of the Nd^{3+} emissions relative to those of complex **1** were also obtained, respectively. From the viewpoint of the energy level match, in spite of the effective energy transfer taking place in complexes **1** and **3**, the smaller energy gap between the energy-donating ^3LC level (18382 cm^{-1}) of the $(\text{HL}^2)^-$ ligand and the emitting level ($^4\text{I}_{1/2}$, 9424 cm^{-1}) for complex **3** than that between the energy-donating ^3LC level (18692 cm^{-1}) of the $(\text{HL}^1)^-$ ligand and the emitting level ($^4\text{I}_{1/2}$, 9217 cm^{-1}), results in the lower non-radiative energy loss during the energy transfer, which should be the reason to the enhanced NIR luminescence of complex **3**.

Conclusions

In conclusion, with the compound $[\text{Zn}(\text{HL}^1)_2(\text{Py})]$ or $[\text{Zn}(\text{HL}^2)_2(\text{Py})]$ from the respective benzimidazole-based ligand H_2L^1 or H_2L^2 as the precursor, series of hetero-binuclear Zn–Ln complexes

$[\text{ZnLn}(\text{HL}^1)_2(\text{Py})(\text{NO}_3)_3]$ ($\text{Ln} = \text{Nd}$, **1** or $\text{Ln} = \text{Gd}$, **2**) and $[\text{ZnLn}(\text{HL}^2)_2(\text{Py})(\text{NO}_3)_3]$ ($\text{Ln} = \text{Nd}$, **3** or $\text{Ln} = \text{Gd}$, **4**) with two energy donors around the Ln^{3+} ion are obtained, respectively. The results of their photophysical studies show that the strong and characteristic NIR luminescence of Nd^{3+} ions with emissive lifetimes in the microsecond range, has been sensitized from the excited state (both ^1LC and ^3LC) of the benzimidazole-based ligand due to the effective intramolecular energy transfer, and the involvement of heavy atoms (Br) at the ligand endows the enhanced NIR luminescent property. While in facilitating the NIR sensitization, the specific design of hetero-metallic polynuclear complexes from the benzimidazole-based ligands is now under way.

Acknowledgements

This work is funded by the National Natural Science Foundation (21173165, 20871098), the Program for New Century Excellent Talents in University from the Ministry of Education of China (NCET-10-0936), the research fund for the Doctoral Program (20116101110003) of Higher Education of China, the State Key Laboratory of Structure Chemistry (20100014), the Provincial Natural Foundation (2011JQ2011) of Shaanxi, the Education Committee Foundation of Shaanxi Province (11JK0588), Hong Kong Research Grants Council (HKBU 202407 and FRG/06-07/II-16) in P. R. of China, the Robert A. Welch Foundation (Grant F-816), the Texas Higher Education Coordinating Board (ARP 003658-0010-2006) and the Petroleum Research Fund, administered by the American Chemical Society (47014-AC5).

Appendix A. Supplementary data

Supplementary data associated with this article can be found, in the online version, at <http://dx.doi.org/10.1016/j.saa.2012.08.048>.

References

- [1] J.-C.G. Bünzli, Chem. Rev. 110 (2010) 2729–2755.
- [2] (a) J. Kido, Y. Okamoto, Organo lanthanide metal complexes for electroluminescent materials, Chem. Rev. 102 (2002) 2357–2368; (b) J.-C.G. Bünzli, S.V. Eliseeva, J. Rare Earths 28 (2010) 824–842.
- [3] S. Comby, J.-C.G. Bünzli, in: K.A. Gschneidner Jr., J.-C.G. Bünzli, V.K. Pecharsky (Eds.), Handbook on the Physics and Chemistry of Rare Earths, vol. 37, Elsevier Science B.V., Amsterdam, 2007. Chapter 235.
- [4] J.-C.G. Bünzli, C. Piguet, Chem. Soc. Rev. 34 (2005) 1048–1077.
- [5] (a) M.D. Ward, Coord. Chem. Rev. 251 (2007) 1663–1677; (b) F.-F. Chen, Z.-Q. Chen, Z.-Q. Bian, C.-H. Huang, Coord. Chem. Rev. 254 (2010) 991–1010; (c) M.D. Ward, Coord. Chem. Rev. 254 (2010) 2634–2642.
- [6] L. Winkless, R.H.C. Tan, Y. Zheng, M. Motevalli, P.B. Wyatt, W.P. Gillin, Appl. Phys. Lett. 89 (2006) 11115–1–3.
- [7] C.M.G. dos Santos, A.J. Harte, S.J. Quinn, T. Gunnlaugsson, Coord. Chem. Rev. 252 (2008) 2512–2527.
- [8] (a) W.-K. Wong, H.Z. Liang, W.-Y. Wong, Z.W. Cai, K.-F. Li, K.-W. Cheah, New J. Chem. 26 (2002) 275–278; (b) W.-K. Lo, W.-K. Wong, J.P. Guo, W.-Y. Wong, K.-F. Li, K.-K. Cheah, Inorg. Chim. Acta 357 (2004) 4510–4521; (c) X.P. Yang, R.A. Jones, Q.Y. Wu, M.M. Oye, W.-K. Lo, W.-K. Wong, A.L. Jolmes, Polyhedron 25 (2006) 271–278; (d) W.-K. Lo, W.-K. Wong, W.-Y. Wong, J.-P. Guo, K.-T. Yeung, Y.-K. Cheng, X.P. Yang, R.A. Jones, Inorg. Chem. 45 (2006) 9315–9325; (e) W.Y. Bi, X.Q. Lü, W.L. Chai, J.R. Song, W.-K. Wong, X.P. Yang, R.A. Jones, Z. Anorg. Allg. Chem. 634 (2008) 1795–1800; (f) W.Y. Bi, X.Q. Lü, W.L. Chai, W.J. Jin, J.R. Song, W.-K. Wong, Inorg. Chem. Commun. 11 (2008) 1316–1319; (g) W.Y. Bi, X.Q. Lü, W.L. Chai, J.R. Song, W.-Y. Wong, W.-K. Wong, R.A. Jones, J. Mol. Struct. 891 (2008) 450–455.
- [9] (a) W.Y. Bi, T. Wei, X.Q. Lü, Y.N. Hui, J.R. Song, W.-K. Wong, R.A. Jones, New J. Chem. 33 (2009) 2326–2334; (b) W.X. Feng, Y.N. Hui, T. Wei, X.Q. Lü, J.R. Song, Z.N. Chen, S.S. Zhao, W.-K. Wong, R.A. Jones, Inorg. Chem. Commun. 14 (2011) 75–78; (c) Y.N. Hui, W.X. Feng, T. Wei, X.Q. Lü, J.R. Song, S.S. Zhao, W.-K. Wong, R.A. Jones, Inorg. Chem. Commun. 14 (2011) 200–204.
- [10] X.Q. Lü, W.X. Feng, Y.N. Hui, T. Wei, J.R. Song, S.S. Zhao, W.-Y. Wong, W.-K. Wong, R.A. Jones, Eur. J. Inorg. Chem. (2010) 2714–2722.

- [11] F.Z.C. Fellah, J.-P. Costes, C. Duhayon, J.-C. Daran, J.-P. Tuchagues, *Polyhedron* 29 (2010) 2111–2119.
- [12] (a) X.P. Yang, R.A. Jones, M.J. Wiester, M.M. Oye, W.-K. Wong, *Cryst. Growth Des.* 10 (2010) 970–976;
(b) X.-P. Yang, R.A. Jones, M.M. Oye, M. Wiester, R.J. Lai, *New J. Chem.* 35 (2011) 310–318.
- [13] G.M. Sheldrick, *SHELXS-97: Program for crystal structure refinement*; Göttingen, Germany, 1997.
- [14] G.M. Sheldrick, *SADABS*, University of Göttingen, 1996.
- [15] (a) V. Bertolasi, P. Gilli, V. Ferretti, G. Gilli, *J. Am. Chem. Soc.* 113 (1991) 4917–4925;
(b) P. Gilli, V. Bertolasi, V. Ferratti, G. Gilli, *J. Am. Chem. Soc.* 122 (2000) 10405–10417.
- [16] S. Petoud, S.M. Cohen, J.-C.G. Bünzli, K.N. Raymond, *J. Am. Chem. Soc.* 125 (2003) 13324–13325.
- [17] M.J. Weber, *Phys. Rev.* 171 (1968) 283–291.
- [18] J.-C.G. Bünzli, *Science*, in: J.-C.G. Bünzli, G.R. Choppin (Eds.), *Lanthanide Probe in life, Lanthanide Probe in life, Chemical and Earth Sciences, Theory and Practice*, Elsevier Science Publ. B.V., Amsterdam, 1989, pp. 219–293. Chapter 7.
- [19] W.T. Carnall, P.R. Fields, K. Rajnak, *J. Chem. Phys.* 49 (1968) 4443–4446.
- [20] D.L. Dexter, *J. Chem. Phys.* 21 (1953) 836–850.
- [21] (a) M. Albrecht, O. Ossetska, J. Klankermayer, R. Fröhlich, F. Gumy, J.-C.-G. Bünzli, *Chem. Commun.* (2007) 1834–1836;
(b) E.G. Moore, A.P.S. Samuel, K.N. Raymond, *Acc. Chem. Res.* 42 (2008) 542–552.